# Orthologous Divergence and Paralogous Anticonvergence in Molecular Evolution of Triplicated Green Opsin Genes in Medaka Fish, Genus *Oryzias*

Yoshifumi Matsumoto[1,2,*], Shoji Oda[1], Hiroshi Mitani[1], and Shoji Kawamura[1,*]

[1]Department of Integrated Biosciences, Graduate School of Frontier Sciences, The University of Tokyo, Kashiwa, Chiba, Japan

[2]Live Imaging Center, Central Institute for Experimental Animals (CIEA), Kawasaki, Kanagawa, Japan

*Corresponding authors: E-mails: kawamura@edu.k.u-tokyo.ac.jp; miraihe13@ciea.or.jp.

**Accepted:** 25 May 2020

**Data deposition:** New sequence data have been deposited at GenBank/DDBJ/EMBL under the accession LC260048–LC260059 (supplementary table S4, Supplementary Material online).

## Abstract

Gene duplication of green (RH2) opsin genes and their spectral differentiation are well documented in many teleost fish. However, their evolutionary divergence or conservation patterns among phylogenetically close but ecologically diverse species is not well explored. Medaka fish (genus *Oryzias*) are broadly distributed in fresh and brackish waters of Asia, with many species being laboratory-housed and feasible for genetic studies. We previously showed that a Japan strain (HNI) of medaka (*Oryzias latipes*) possessed three RH2 opsin genes (*RH2-A*, *RH2-B*, and *RH2-C*) encoding spectrally divergent photopigments. Here, we examined the three RH2 opsin genes from six *Oryzias* species representing three species groups: the *latipes*, the *celebensis*, and the *javanicus*. Photopigment reconstitution revealed that the peak absorption spectra ($\lambda_{max}$) of RH2-A were divergent among the species (447–469 nm), whereas those of RH2-B and RH2-C were conservative (516–519 and 486–493 nm, respectively). For the RH2-A opsins, the largest spectral shift was detected in the phylogenetic branch leading to the *latipes* group. A single amino acid replacement T94C explained most of the spectral shift. For RH2-B and -C opsins, we detected tracts of gene conversion between the two genes homogenizing them. Nevertheless, several amino acid differences were maintained. We showed that the spectral difference between the two opsins was attributed to largely the E/Q amino acid difference at the site 122 and to several sites with individually small spectral effects. These results depict dynamism of spectral divergence of orthologous and paralogous green opsin genes in phylogenetically close but ecologically diverse species exemplified by medaka.

**Key words:** RH2 opsin, absorption spectra, spectral tuning, gene duplication, gene conversion, natural selection.

## Introduction

Opsin genes responsible for color vision form a gene family created by gene duplications. Vertebrate cone opsins are classified into four phylogenetic types in vertebrates with different spectral sensitivities expressed in cone photoreceptor cells in the retina: SWS1 sensitive roughly to ultraviolet to violet, SWS2 to blue, RH2 to green, M/LWS to green to red ranges of the light wavelength (Yokoyama 2000). Teleost fish are unique among vertebrates in that the four types of opsin genes are often further duplicated to create diverse sets of subtypes (Chinen et al. 2003; Fuller et al. 2004; Parry et al. 2005; Matsumoto et al. 2006; Watson et al. 2011; Nakamura et al. 2013; Kasagi et al. 2015; Musilova et al. 2019). The reported subtypes are often differentiated in spectral sensitivity and spatiotemporal expression pattern in the retina presumably adapting to varying photic environments in water (Takechi and Kawamura 2005; Carleton et al. 2008; Kawamura et al. 2016; Mackin et al. 2019).

Among the four opsin types, the RH2 type appears to have experienced the largest number of gene duplication events (Spady et al. 2006; Rennison et al. 2012). The evolutionary rate of RH2 opsins in euteleost lineages is accelerated by 5- to 6-fold from that in the early vertebrate ancestors (Yokoyama and Tada 2010), implying that RH2 opsins of teleosts have

evolved in quite a dynamic fashion. Thus, RH2 opsins would be suitable for studying evolutionary fate and adaptation of duplicated opsin genes by examining their divergence or conservation patterns among phylogenetically close but ecologically diverse species, which is, however, not well explored.

The medaka (genus *Oryzias*), also known as ricefish, ranges broadly throughout fresh and brackish waters of Central, South, Southeast to East Asia, and the Indo-Malay-Philippines Archipelago as far east as Timor, and are currently classified into 24 species (Naruse 1996; Parenti 2008). *Oryzias* species can be divided into three major species groups, the *latipes*, *celebensis*, and *javanicus* groups (Takehana et al. 2005). Because of small size, relatively large and clear eggs, ease of maintenance in freshwater aquaria, and other reasons, the Japanese medaka (*Oryzias latipes*) has been one of the most widely used species in experimental biology and is one of the three most important model organisms among bony fish along with the zebrafish, *Danio rerio* and the pufferfish, *Takifugu rubripes* (Wittbrodt et al. 2002; Kasahara et al. 2007; Parenti 2008). Many *Oryzias* species are laboratory-housed and feasible for genetic studies (Iwamatsu et al. 1993; Matsuyama 1994; Katsumura et al. 2009; Matsumoto et al. 2009).

We previously examined a northern Japan strain, HNI, of *O. latipes* and showed that it possessed three RH2 opsin genes (*RH2-A*, *RH2-B*, and *RH2-C*) arrayed in tandem in the genome and encoding spectrally divergent photopigments with peak absorption spectra ($\lambda_{max}$) at 452, 516, and 492 nm, respectively (Matsumoto et al. 2006). Although the northern and southern populations of Japanese medaka are classified as the same species, being able to breed to produce healthy and fertile offspring, their split is estimated to be as deep as human–chimpanzee to human–orangutan splits, 4–18 Ma, and would have resulted in a genetic divergence with sufficient resolution for molecular evolutionary analyses (Takehana et al. 2003; Setiamarga et al. 2009). Thus, *Oryzias* species are suitable for the study of divergence or conservation patterns of the RH2 opsin gene among phylogenetically close (congeneric) but ecologically diverse species. In the present study, we examined the RH2 opsin genes of six species of *Oryzias* representing the three species groups: a southern Japan strain, Hd-rR, of *O. latipes* and Philippine medaka (*Oryzias luzonensis*) from the *latipes* group; Celebes ricefish (*Oryzias celebensis*) and Sarasins' buntingi (*O. sarasinorum*) from the *celebensis* group; deep-bodied ricefish (*Oryzias melastigma*) and dwarf medaka (*Oryzias minutillus*) from the *javanicus* group (Formacion and Uwa 1985; Roberts 1998; Parenti and Soeroto 2004; Parenti 2008) (table 1).

## Materials and Methods

### Fish Samples

Five *Oryzias* species (*O. luzonensis*, *O. celebensis*, *O. sarasinorum*, *O. melastigma*, and *O. minutillus*) were obtained from laboratory stocks supplied by NBRP Medaka (https://shigen.nig.ac.jp/medaka/, last accessed June 6, 2020) and maintained at the University of Tokyo. The University of Tokyo Animal Care and Use Committee approved all animal protocols (approval number C-14-01) in accordance with the Code of Ethics of the World Medical Association (Declaration of Helsinki).

### DNA Cloning

Using the total RNA prepared from eyes of an adult fish, the first-strand cDNA was synthesized by using a poly (dT) primer (5′-aagcagtggtaacaacgcagagtact(30)vn-3′) (v: a, g, or c; n: a, g, c, or t; t(30): 30 succession of t). Opsin cDNAs were PCR-amplified using primer pairs (supplementary table S1, Supplementary Material online) which were designed based on the published nucleotide sequences of *RH2-A*, *RH2-B*, and *RH2-C* genes of *O. latipes* (HNI strain) (Matsumoto et al. 2006). Next, the 5′ and 3′ rapid amplification of cDNA ends (RACE) was carried out to reveal their untranslated regions and full-length coding sequences by using primer pairs specific to the species and genes (supplementary table S2, Supplementary Material online). The genomic sequences of the three genes including introns were determined for the same individuals with those examined for cDNA sequences using primers designed for photopigment reconstitution (supplementary table S3, Supplementary Material online). The PCR products were cloned into the pBluescript II (SK-) plasmids. All PCR products were sequenced in both strands using ABI PRISM 3130-Avant Genetic Analyzer (Applied Biosystems Japan, Tokyo, Japan). The DNA sequences were confirmed in duplicate PCRs.

### Phylogenetic Tree

Alignment of deduced amino acid sequences was carried out using CLUSTAL W (Thompson et al. 1994) and refined visually. Coding nucleotide sequences were aligned in accordance with the protein alignments. Evolutionary distance was estimated using the Tamura–Nei algorithm (Tamura and Nei 1993). Phylogenetic tree was reconstructed using the neighbor-joining method (Saitou and Nei 1987). The reliability of the tree topology was evaluated by the bootstrap analysis with 1,000 replications (Felsenstein 1985). All these analyses were conducted using a program package MEGA X (Kumar et al. 2018).

### Reconstitution of Opsin Photopigment

The opsin cDNAs were recloned into the pMT5 expression vector which contained the last 15 amino acids of the bovine rhodopsin necessary for immunoaffinity purification by 1D4 monoclonal antibody (Kawamura and Yokoyama 1998). The PCR primer pairs (supplementary table S3, Supplementary Material online) for the recloning contain the 5′- and 3′-edges

**Table 1**
Distribution and Habitat of Study Species of *Oryzias*

| Species Group | Species Name | Distribution | Habitat |
|---|---|---|---|
| *latipes* | *Oryzias latipes* | Eastern China, east Korea, Japanese Archipelago | Fresh to brackish water |
| | *Oryzias luzonensis* | Luzon Island | Creeks and rice fields |
| *celebensis* | *Oryzias celebensis* | South-western arm of Sulawesi, Lake Tempe, East Timor, River Mota Talau area | Inland and coastal rivers and streams |
| | *Oryzias sarasinorum* | Central Sulawesi, Lake Lindu | Pelagic open waters |
| *javanicus* | *Oryzias melastigma* | India, Sri Lanka, Bangladesh, and Myanmar | Coastal brackish and freshwater |
| | *Oryzias minutillus* | Chao Phrya basin and Salween basins, Mekong basin in northern Thailand and Kampuchea, Yunnan Province of China | Clear water swamps |

of the coding regions with necessary restriction sites for cloning and the Kozak sequence for efficient translation (Kawamura and Yokoyama 1998). The nucleotide sequences of the pMT5-cDNA clones were confirmed to match those of the template pBluescript-cDNA clones.

Point mutations were introduced by using QuikChange site-directed mutation kit (Stratagene, La Jolla, CA). All mutagenized cDNAs were sequenced in both strands using ABI PRISM 3130-Avant Genetic Analyzer (Applied Biosystems Japan, Tokyo, Japan).

The pMT5-cDNA clones were expressed in cultured COS-1 cells (RIKEN Cell Bank, Tsukuba, Japan). The cells were incubated with 5 $\mu$M 11-*cis* retinal (Storm Eye Institute, Medical University of South Caroline, Charleston, SC) and solubilized with 1% dodesyl maltoside (Anatrace, Maumee, OH). Produced photopigments were purified using the immobilized 1D4 monoclonal antibody (Cell Culture Center, Minneapolis, MN) as in previous studies (Chinen et al. 2003; Matsumoto et al. 2006). UV-visible absorption spectra of the photopigments were measured using U3010 dual-beam spectrometer (Hitachi, Tokyo, Japan) at 20 °C for at least five times in the dark and for at least five more times after 3 min of light exposure.

### Inference of Ancestral Amino Acid Sequences of RH2-A Opsins

The ancestral amino acid sequence at each ancestral node was inferred by using phylogenetic analysis by maximum likelihood (PAML) computer program version 4.8 with a likelihood-based Bayesian method (http://abacus.gene.ucl.ac.uk/software/paml.html, last accessed June 6, 2020) (Yang et al. 1995; Yang 2007).

In order to infer the ancestral amino acid sequence of the *RH2-A* opsins among *Oryzias* species, the following RH2 opsin genes were used as outgroups: *O. latipes* (HNI) *RH2-B* (GenBank accession number: AB223054) and *RH2-C* (AB223055), a cichlid (*Pseudotropheus acei*) *RH2B* (DQ088645), *RH2A*$\alpha$ (DQ088630) and *RH2A*$\beta$ (DQ088633), Nile tilapia (*Oreochromis niloticus*) *RH2B* (JF262086), pufferfish (*T. rubripes*) *RH2* (NM001033712), tetraodon (*Tetraodon nigroviridis*) *RH2* (AY598944), rainbow trout (*Oncorhynchus mykiss*) *RH2* (AF425076), Atlantic salmon (*Salmo salar*) *RH2* (AY214132), zebrafish (*D. rerio*) *RH2-1* (AB087805), *RH2-2* (AB087806), *RH2-3* (AB087807) and *RH2-4* (AB087808), goldfish (*Carassius auratus*) *GFgr1* (L11865) and *GFgr2* (L11866), and Carp (*Cyprinus carpio*) gr-*1* (AB110602) and *gr-2* (AB110603).

### Inference of Positive Selection in *RH2-A* Opsin Genes

To explore selective constraint of RH2-A opsin genes, same phylogenetic trees with inference of ancestral amino acid sequence of RH2-A opsin genes were used. Branch-site model, which was performed by the codeml program of the PAML 4.8 software package, allows the $\omega$ ratio to vary among sites along branches on the tree, such that positive selection can be detected in specific codon sites along particular lineages of interest. For branch-site model, Model A test was applied (Yang 2007; Yang and Dos Reis 2011), which estimates $\omega_0$ between 0 and 1 (site under purifying selection) and $\omega_1$=1 (sites evolving neutrally) for sites along all branches, as well as $\omega_{2a}$ (sites under positive selection in the foreground branch but under purifying selection on the background branch) and $\omega_{2b}$ (sites under positive selection in the foreground branch, which are evolving neutrally on the background branch). The likelihood ratio tests were performed between the Model A and the null Model A, which is the same Model A but with $\omega_2$=1 fixed. Likelihood ratio tests were carried out by comparing twice the difference in ln likelihood scores of nested models against the number of extra parameters estimated by the more complex model. The Bayes Empirical Bayes calculation of posterior probabilities for site classes was used to calculate the probabilities of sites under positive selection.

## Results

### Phylogeny of *Oryzias* RH2 Opsin Genes

The cDNA and genomic sequences were determined for *RH2-A*, *RH2-B*, and *RH2-C* of *O. luzonensis*, *O. celebensis*, *O. sarasinorum*, *O. melastigma*, and *O. minutillus* (see

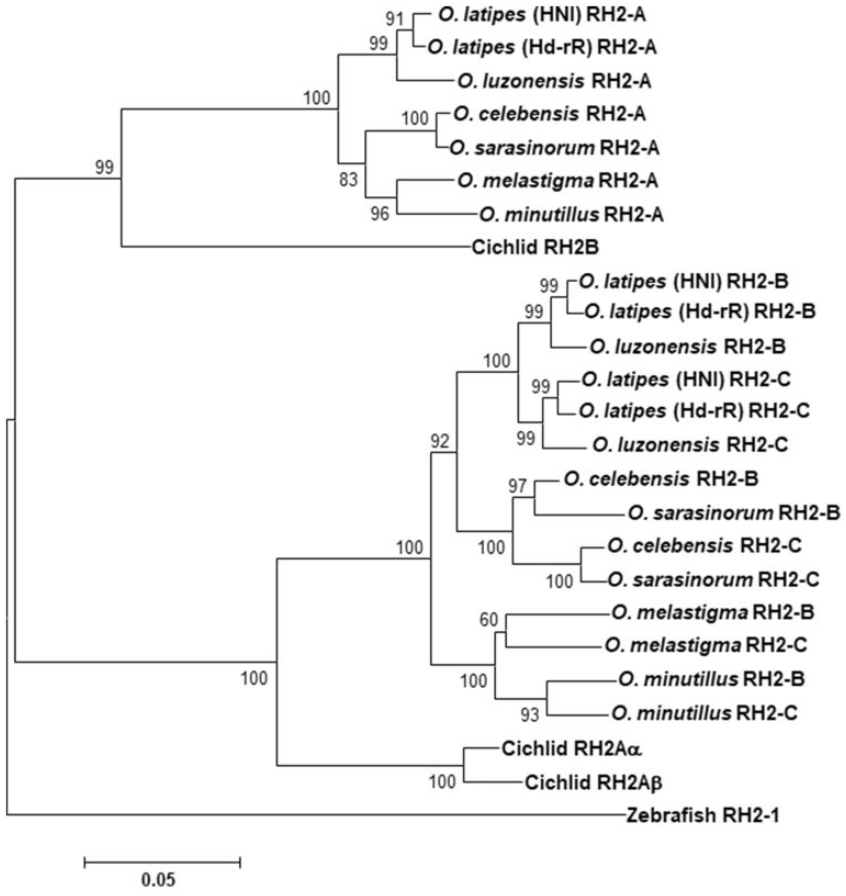


**Fig. 1.**—A phylogenetic tree reconstructed for the RH2 opsin genes of medaka (*Oryzias*) species using entire coding nucleotide sequences. A cichlid (*Melanochromis vermivorus*) *RH2B* (GenBank accession number: DQ088646) was added to the analysis as an outgroup of *Oryzias RH2-A* genes (Parry et al. 2005). Its *RH2Aα* (DQ088631) and *RH2β* (DQ088634) were also included as an outgroup of medaka *RH2-B/C* gene cluster (Parry et al. 2005). The zebrafish (*Danio rerio*) *RH2-1* (AB087805) was added as an outgroup to the medaka/cichlid RH2 genes (Chinen et al. 2003). The bootstrap percentages are given to each node. Scale bar: five nucleotide substitutions per 100 sites.

supplementary tables S1–S3, Supplementary Material online, for relevant PCR primers). GenBank accession numbers of these nucleotide sequences are listed in supplementary table S4, Supplementary Material online. Regarding Hd-rR strain of *O. latipes*, nucleotide sequences of the three genes were retrieved from the whole genome sequence data (Kasahara et al. 2007) (supplementary fig. S1, Supplementary Material online).

Figure 1 shows a phylogenetic relationship reconstructed using coding nucleotide sequences among the *Oryzias* RH2 opsin genes including those of HNI (Matsumoto et al. 2006) with outgroup sequences from cichlid and zebrafish. All of the *RH2-A* sequences determined in this study clustered with those of HNI and Hd-rR strains of *O. latipes* and with the cichlid ortholog *RH2B* located outside of the *Oryzias RH2-A*s as expected from previous studies (Matsumoto et al. 2006; Spady et al. 2006). Similarly, all the *RH2-B* and *RH2-C* sequences determined in this study clustered with those of HNI and Hd-rR and with the cichlid *RH2Aα* and *RH2Aβ*.

## Gene Conversion between *RH2-B* and *RH2-C*

In figure 1, *RH2-B* and *RH2-C* genes clustered by species group or by species as if they arose in the common ancestor of *O. latipes* and *O. luzonensis* (*latipes* group), in that of *O. celebensis* and *O. sarasinorum* (*celebensis* group), in *O. melastigma* and in *O. minutillus* by independent gene duplications. To test if this topology of the gene tree is due to sequence homogenization by gene conversions between the two genes, we applied GENECONV (Sawyer 1989) to the two genes in each *Oryzias* species (fig. 2*A* and supplementary table S5, Supplementary Material online). GENECONV searches for a consecutively identical region between two sequences and evaluates the probability of achieving homogeneity when we assume nucleotide differences to distribute randomly throughout the sequence region. An orthologous region corresponding to the nucleotide position 300 to position 918 in *RH2-B* of the *O. latipes* (HNI) appeared less affected by gene conversion (fig. 2*A*). In the reconstructed gene tree with

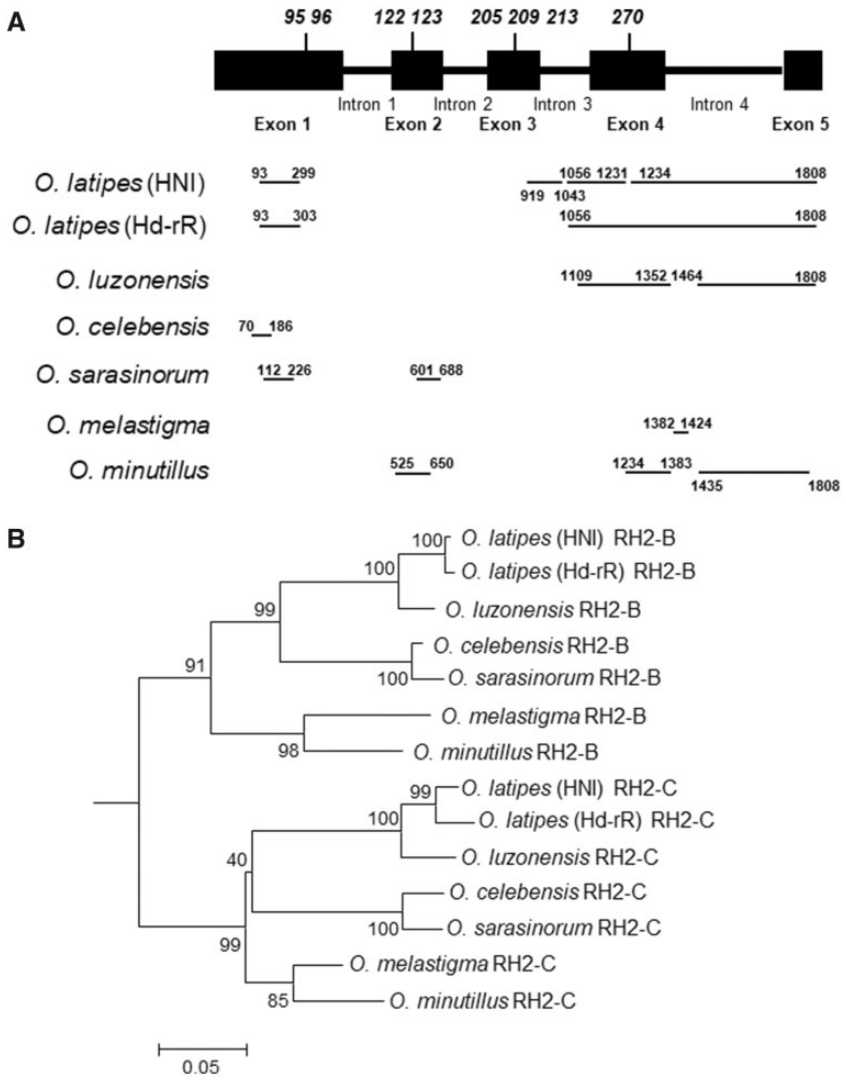


**Fig. 2.**—The gene conversion and the origin of the gene duplication on the *RH2-B* and *RH2-C* opsin genes of *Oryzias* species. (*A*) Distribution of gene conversions inferred by GENECONV. The exon–intron structure of the RH2 opsin genes is indicated at the top. The italic numbers above the exon boxes represent amino acid site numbers highlighted in figure 5. The horizontal lines beside species names represent the area covered by gene conversions inferred for the pairs of *RH2-B* and *RH2-C* opsin genes. The numbers indicated at edges of the lines correspond to the nucleotide site number represented by *RH2-B* of *O. latipes* (HNI) which is counted from its first nucleotide of the start codon throughout the gene region including introns. GENECONV program version 1.81 was obtained through https://www.math.wustl.edu/~sawyer/geneconv/ (last accessed June 6, 2020). (*B*) A phylogenetic tree of *Oryzias RH2-B* and *RH2-C* genes supporting a gene duplication deriving the two genes in the common ancestor of the *Oryzias* species. The nucleotide position 300–918 in figure 2*A* was used. As an outgroup, *RH2-A* of the *O. latipes* (Hd-rR) was used to locate a phylogenetic root to the tree. The bootstrap percentages are given to each node. Scale bar: five nucleotide substitutions per 100 sites.

this region (fig. 2*B*), *RH2-B* sequences and *RH2-C* sequences clustered, respectively, supporting that the gene duplication occurred only once in the common ancestor of *Oryzias* species. If a gene duplication occurred in the common ancestor, we can explain the appearance of multiple gene duplications in the tree by postulating gene conversions in each species. On the contrary, if gene duplications occurred in multiple species, we cannot explain the gene-tree topology in figure 2*B* unless postulating multiple parallel mutations or horizontal gene transfer between species which is unrealistic. Thus, the gene duplication that derived *RH2-B* and *RH2-C* must have occurred only once in the common ancestor of *Oryzias* species.

## Absorption Spectra of *Oryzias* RH2 Opsins

Absorption spectra were measured for *Oryzias* RH2 opsin photopigments (supplementary table S6, Supplementary Material online and fig. 3). The spectra in the dark had a prominent absorption peak in addition to a protein absorbance at 280 nm. When the reconstituted pigments were exposed to light, a new absorption peak appeared at

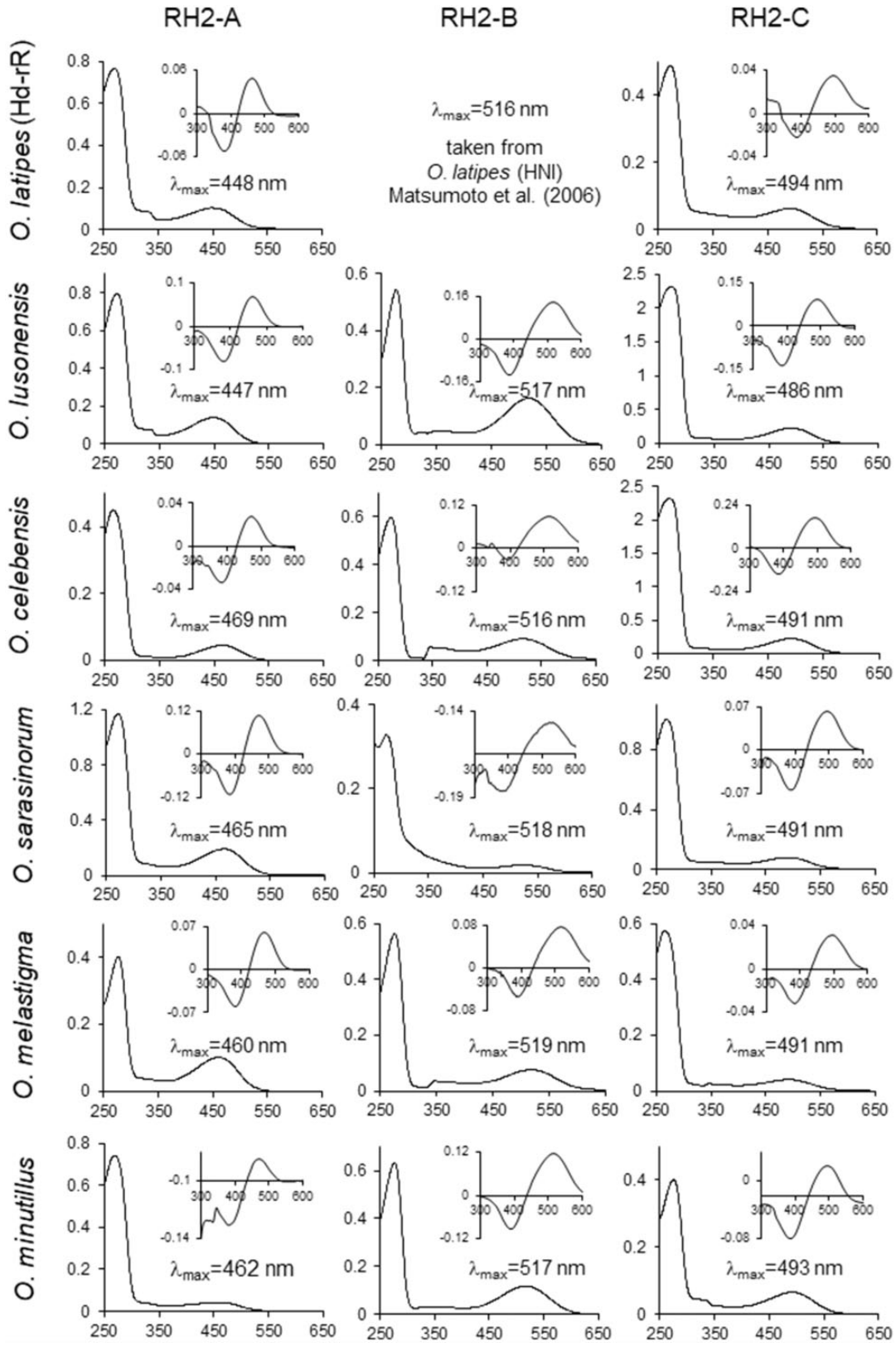


**Fig. 3.**—Absorption spectra of the reconstituted *Oryzias* RH2 opsin photopigments measured in the dark. The dark–light difference spectra are given in insets. $\lambda_{max}$ values are taken from the dark spectra. Because the amino acid sequence of the RH2-B opsin of *O. latipes* (Hd-rR) was identical with that of *O. latipes* (HNI), the $\lambda_{max}$ value of Hd-rR RH2-B was taken from the published information on HNI RH2-B.

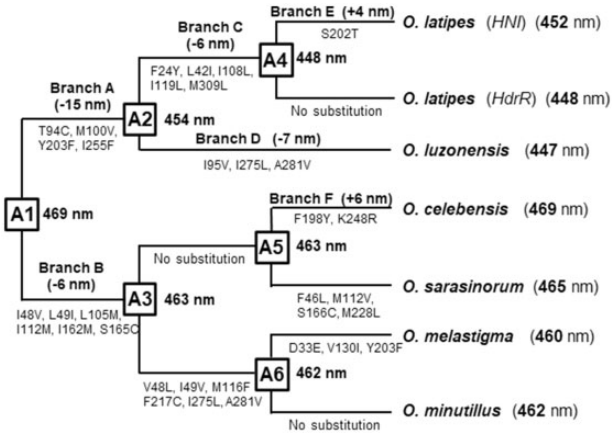


**Fig. 4.**—Amino acid substitutions inferred on the phylogenetic branches connecting ancestral and contemporary sequences of *Oryzias* RH2-A opsins. The $\lambda_{max}$ values of contemporary opsins are indicated beside species names. The $\lambda_{max}$ values of ancestral opsins are indicated at nodes A1–A6. The magnitude of spectral shifts ≥4 nm is indicated in parentheses with branch names (Branches A–F).

380 nm represented as a negative peak in the dark–light difference spectra indicated in the insets of figure 3. This indicates that 11-*cis* retinal in the pigments was isomerized by light and all-*trans* retinal was released. These results demonstrate that the reconstituted pigments were in fact photoreactive. $\lambda_{max}$ values of RH2-A opsins were divergent among species, ranging from 447 nm (*O. luzonensis*) to 469 nm (*O. celebensis*). In contrast, the $\lambda_{max}$ values of RH2-B and RH2-C opsins were conservative, ranging from 516 to 519 nm and from 486 to 494 nm, respectively.

## Evolutionary Process of Spectral Divergence among *Oryzias* RH2-A Opsins

To elucidate amino acid changes responsible for the spectral divergence among the *Oryzias* RH2-A opsins (supplementary fig. S2, Supplementary Material online), we inferred their ancestral amino acid sequences (supplementary fig. S3, Supplementary Material online) at phylogenetic-tree nodes Ancestor 1 (A1)–Ancestor 6 (A6) (fig. 4). We assumed their phylogenetic relationship depicted in figure 1 which is consistent with a previous study (Takehana et al. 2005) where combined nuclear and mitochondrial sequence data were analyzed. Under both Dayhoff (Dayhoff et al. 1978) and JTT models (Jones et al. 1992), average posterior probability over entire amino acid sites was 0.99 in all the six ancestral sequences. The two sets of amino acid sequences were identical except at two sites (49th and 100th: the residue numbering follows that of bovine rhodopsin as a standard in all RH2 opsins throughout this article) in A1 with leucine (Dayhoff) or isoleucine (JTT) at 49th and methionine (Dayhoff) or valine (JTT) at 100th. Based on the Dayhoff model, amino acid substitutions are plotted on the phylogenetic branches in figure 4.

Amino acid sequences were identical between A3 and A5, between A4 and *O. latipes* (Hd-rR), and between A6 and *O. minutillus*. We thus reconstituted photopigments for A1, A2, and A3 and measured their absorption spectra (supplementary table S7 and fig. S4, Supplementary Material online). A2 was created by introducing three amino acid changes (V95I [valine to isoleucine at residue 95], L275L, V281A) into *O. luzonensis* RH2-A. A1 was created from A2 by introducing four amino acid changes (C94T, V100M, F203Y, F255I). A3 (= A5) was created by introducing two amino acid changes (Y198F, R248K) to *O. celebensis* RH2-A. We also created the JTT-version of A1 by introducing L49I and M100V to the Dayhoff-version of A1. The $\lambda_{max}$ of the JTT-version of A1 was 467.0 ± 0.5 nm. Since the difference from the Dayhoff-version was negligible (1.7 nm), only the Dayhoff-version is used hereafter.

The largest spectral shift occurred in Branch A from A1 to A2 (−15 nm) toward the *latipes* group (*O. latipes* and *O. luzonensis*) (fig. 4). In the *latipes* group, further shortwave shifts occurred in Branch C (−6 nm toward *O. latipes*) and in Branch D (−7 nm toward *O. luzonensis*). *Oryzias latipes* HNI shifted oppositely for long wave with +5 nm. Toward the *celebensis* group and the *javanicus* group, spectral shift was moderate: −6 nm from A1 to A3 (the common ancestor of the two species groups) in Branch B with little shift thereafter except in Branch F toward *O. celebensis* with +6 nm longwave shift.

## Complex Spectral Effects of Amino Acid Changes in *Oryzias* RH2-A Opsins

Based on figure 4, we tested effects of the amino acid substitutions on the spectral shift occurred in the evolutionary branches A–F by site-directed mutagenesis (table 2).

In Branch A with −15-nm spectral shift, there were four amino acid changes: T94C, M100V, Y203F, and I255F. A previous study on the newt SWS2 opsin reported a large spectral effect of the site 94 (Takahashi and Ebrey 2003). Indeed, T94C resulted in −20-nm shift (table 2). However, this is larger than the actual spectral shift in this branch (−15 nm). When T94C was combined with single or double other mutations, spectral shifts were still larger. Thus, the spectral shift in Branch A was realized by nonlinear interaction of the four mutations with T94C playing a major role.

In Branch B with − 6-nm shift, there were six amino acid changes: I48V, L49I, L105M, I112M, I162M, and S165C (fig. 4). Although an exhaustive survey was not conducted testing all single mutations and their combinations, the spectral shift was attributable to an additive effect of L105M and I112M in large part (table 2).

In Branch C with −6-nm shift, there were five amino acid changes: F24Y, L42I, I108L, I119L, and M309L (fig. 4). Three of them, L42I, I108L, and M309L, individually resulted in an

**Table 2**
Spectral Effects of Mutations at Each Branch

| | Pigment | λMax± SE (nm) | Δλ from Ancestor |
|---|---|---|---|
| Branch A | Ancestor 1_T94C | 449.0±0.9 | −20 |
| | Ancestor 1_M100V | 467.0±0.6 | −2 |
| | Ancestor 1_T94C/M100V | 448.3±0.7 | −22 |
| | Ancestor 1_T94C/Y203F | 449.7±1.0 | −19 |
| | Ancestor 1_T94C/I255F | 451.0±1.4 | −18 |
| | Ancestor 1_T94C/M100V/Y203F | 450.0±1.5 | −19 |
| | Ancestor 1_T94C/M100V/I255F | 452.0±1.3 | −17 |
| | Ancestor 1_T94C/Y203F/I255F | 449.5±1.5 | −19 |
| Branch B | Ancestor 1_L49I | 468.0±0.3 | −1 |
| | Ancestor 1_L105M | 466.3±1.1 | −2 |
| | Ancestor 1_I112M | 465.7±1.5 | −3 |
| | Ancestor 1_S165C | 468.0±0.4 | −1 |
| | Ancestor 1_I48V/L49I | 466.3±0.4 | −2 |
| | Ancestor 1_L105M/I112M | 463.5±0.4 | −5 |
| | Ancestor 1_I162M/S165C | 467.8±1.0 | −1 |
| Branch C | Ancestor 2_F24Y | 450.7±2.2 | −3 |
| | Ancestor 2_L42I | 447.0±1.0 | −7 |
| | Ancestor 2_I108L | 446.0±1.1 | −8 |
| | Ancestor 2_I119L | 452.0±0.9 | −2 |
| | Ancestor 2_M309L | 447.3±1.8 | −7 |
| Branch D | Ancestor 2_I95V | 452.0±1.1 | −2 |
| | Ancestor 2_I275L | 447.0±1.1 | −7 |
| | Ancestor 2_A281V | 448.0±1.0 | −6 |
| | Ancestor 2_I95V/I275L | 453.0±0.7 | −1 |
| | Ancestor 2_I95V/A281V | 446.0±1.0 | −8 |
| | Ancestor 2_I275L/A281V | 452.0±1.1 | −2 |
| Branch F | Ancestor 5_F198Y | 462.0±0.9 | −1 |
| | Ancestor 5_K248R | 461.0±0.8 | −2 |

enough spectral shift with −7 to −8 nm to explain the −6-nm shift of the branch. The other two also showed minor effects. Thus, nonadditive and regressive interaction among the five changes operates in this branch.

In Branch D with −7-nm shift, there were three amino acid changes: I95V, I275L, and A281V (fig. 4). Two of them, I275L and A281V, individually resulted in an enough spectral shift with −7 and −6 nm, respectively, to explain the −7-nm shift of the branch. But, when these two were combined, spectral shift was only −2 nm. Though I95V showed a minor effect with −2-nm shift, it extinguished the large effect of I275L when combined (−1 nm). Again, nonlinear and regressive interaction among mutations also operates in this branch.

In Branch E with +4-nm shift, there was only one change: S202T (fig. 4). Thus, the spectral shift of the branch should be attributed to this single mutation.

In Branch F with +6-nm shift, there were two amino acid changes: F198Y and K248R (fig. 4). Both mutations caused individually only minor and short-wave shifts with −1 and −2 nm, respectively. Thus, when combined, the two mutations exert a large synergistic effect with opposite wavelength direction from the effect of individual mutation.

## Test of Natural Selection on Spectral Divergence of RH2-A

To explore whether amino acid replacements at Branch A in figure 4 were driven by positive Darwinian selection for functional divergence, we implemented branch-site model in PAML, indicating that the T94C substitution at Branch A was shown to have evolved under positive selection (supplementary table S8, Supplementary Material online).

## Search for Conserved Amino Acid Differences between RH2-B and RH2-C Opsins against Gene Conversion as Key Sites for Their Spectral Distinction

Although the *RH2-B* and *RH2-C* opsin genes are homogenized by gene conversion (figs. 1 and 2), spectral difference is maintained between the RH2-B ($\lambda_{max}$ at 516–519 nm) and RH2-C (486–494 nm) opsins (fig. 3 and supplementary table S6, Supplementary Material online). Among the seven *Oryzias* species/strains (fig. 5), we searched for amino acid sites where in RH2-B opsins residues are same among at least five sequences, and in RH2-C opsins residues are also same among at least five sequences but are different from the major residue in RH2-B opsins. There were such sites in the N-terminal and transmembrane (TM) regions (fig. 5). Since TM regions are in

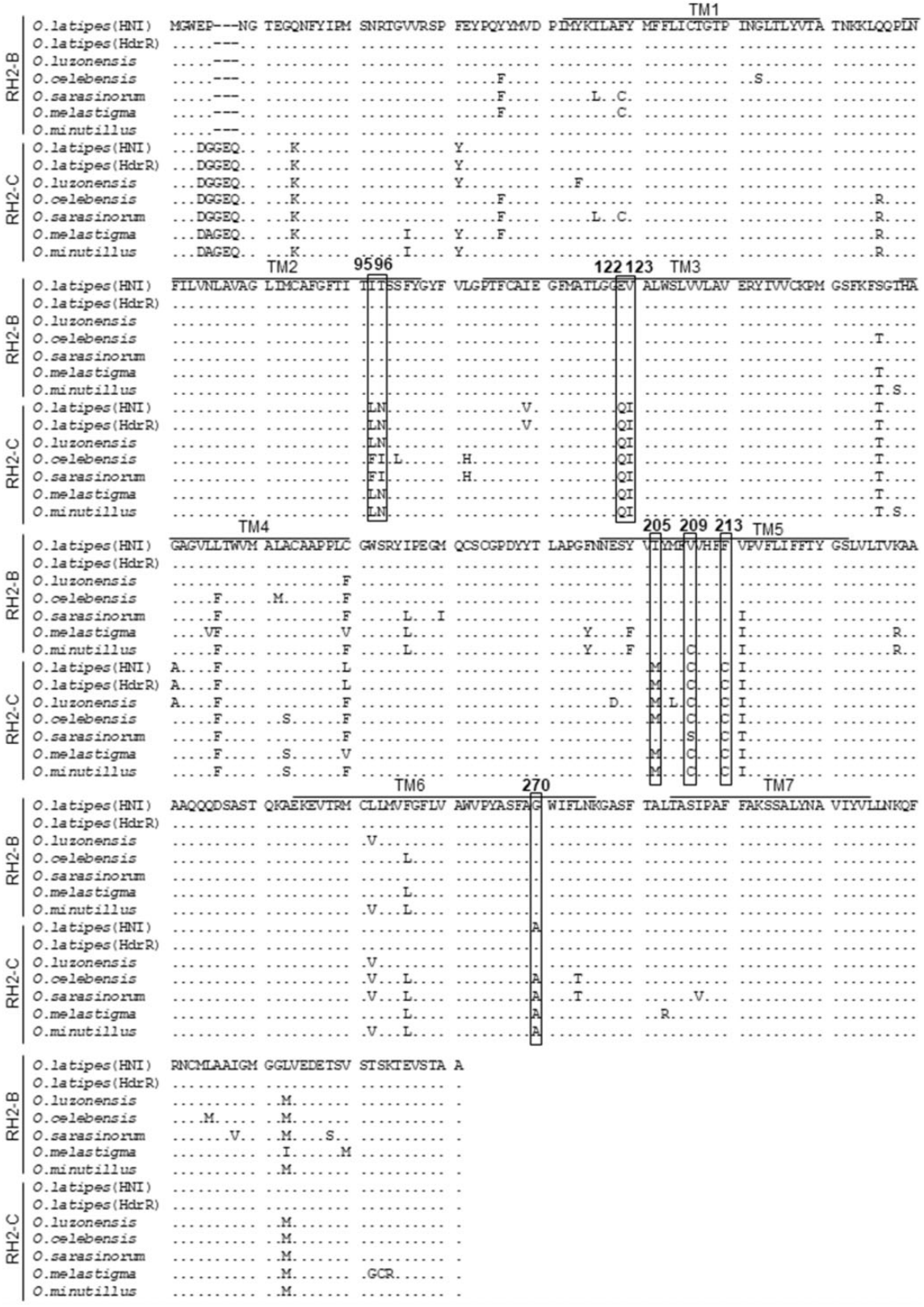


**Fig. 5.**—Aligned amino acid sequences of the RH2-B and RH2-C opsins among *Oryzias* species. Identical amino acids to the *O. latipes* (HNI) RH2-B sequence are indicated by dots. Gap sites are indicated with dashes. The seven transmembrane (TM) domains are indicated by horizontal lines above the *O. latipes* (HNI) RH2-B sequence. The sites 95, 96, 122, 123, 205, 209, 213, and 270 are highlighted by boxes.

**A**

| Opsin | 95 | 96 | 122 | 123 | 205 | 209 | 213 | 270 | $\lambda_{max}$ | $\Delta\lambda_{max}$ from RH2-C |
|---|---|---|---|---|---|---|---|---|---|---|
| RH2-B(●) | I | T | E | V | I | V | F | G | 516.1±0.5 [a] | +24 |
| RH2-C(○) | L | N | Q | I | M | C | C | A | 492.3±0.9 [a] | |

[a] Matsumoto et al. 2006

**B**

| Template | 95 | 96 | 122 | 123 | 205 | 209 | 213 | 270 | $\lambda_{max}$ | $\Delta\lambda_{max}$ from template |
|---|---|---|---|---|---|---|---|---|---|---|
| RH2-C | ● | ● | ● | ● | ● | ● | ● | ● | 516.0±0.2 | +24 |
| RH2-B | ○ | ○ | ○ | ○ | ○ | ○ | ○ | ○ | 493.4±0.8 | −23 |

**C**

| Template | 95 | 96 | 122 | 123 | 205 | 209 | 213 | 270 | $\lambda_{max}$ | $\Delta\lambda_{max}$ from template |
|---|---|---|---|---|---|---|---|---|---|---|
| RH2-C | ○ | ○ | ● | ○ | ○ | ○ | ○ | ○ | 507.9±0.5 | +16 |
| | ● | ○ | ● | ○ | ○ | ○ | ○ | ○ | failed | - |
| | ○ | ● | ● | ○ | ○ | ○ | ○ | ○ | 511.5±0.4 | +20 |
| | ○ | ○ | ● | ● | ○ | ○ | ○ | ○ | 508.2±0.9 | +16 |
| | ○ | ○ | ● | ○ | ● | ○ | ○ | ○ | 508.8±0.4 | +17 |
| | ○ | ○ | ● | ○ | ○ | ● | ○ | ○ | 510.2±0.5 | +18 |
| | ○ | ○ | ● | ○ | ○ | ○ | ● | ○ | 507.8±0.8 | +16 |
| | ○ | ○ | ● | ○ | ○ | ○ | ○ | ● | 508.3±0.4 | +16 |

**FIG. 6.**—Alternation of amino acid composition between RH2-B and RH2-C opsins at sites 95, 96, 122, 123, 205, 209, 213, and 270 in *O. latipes* (HNI). (*A*) The native amino acid compositions of the two opsins. $\lambda_{max}$ values are taken from Matsumoto et al. (2006). Difference of $\lambda_{max}$ ($\Delta\lambda_{max}$) of RH2-B from RH2-C is shown in the right column. (*B*) Exchange of amino acids at all eight sites between RH2-B and RH2-C opsins. Amino acid types in RH2-B are indicate as black dots and those in RH2-C are indicated as white dots. (*C*) Alternation of amino acids at site 122 (top) or at sites 122 and another in RH2-C to those in RH2-B.

the immediate vicinity to the retinal, we focused on the sites in TM: 95, 96, 122, 123, 205, 209, 213, and 270 (highlighted in fig. 5).

Using *O. latipes* (HNI) *RH2-B* and *RH2-C* cDNAs as templates, effects of the amino acid difference at the eight sites on their 24-nm spectral difference were tested by site-directed mutagenesis (fig. 6*A*–*C*). When all eight sites were replaced in the RH2-C template to the RH2-B types (L95I/N96T/Q122E/I123V/M205I/C209V/C213F/A270G), $\lambda_{max}$ shifted to 516.0 ± 0.2 nm which matched well with that of RH2-B (516.1 ± 0.5 nm) (fig. 6*B*). Similarly, when all eight sites were replaced in the RH2-B template to the RH2-C types (I95L/T96N/E122Q/V123I/I205M/V209C/F213C/G270A), $\lambda_{max}$ shifted to 493.4 ± 0.8 nm which matched well with that of RH2-C (492.3 ± 0.9 nm) (fig. 6*B*). Thus, among 21 amino acid differences between RH2-B and RH2-C opsins of *O. latipes* (HNI), these eight amino acid differences are sufficient to explain the spectral difference between them.

Among the eight amino acid sites, E/Q exchange at site 122 is reported to exert a large spectral shift of ∼15 nm in RH2 opsins of Comoran coelacanth (*Latimeria chalumnae*) and zebrafish (Yokoyama et al. 1999; Chinen et al. 2005a). Consistently at this site, E and Q are perfectly conserved in RH2-B and RH2-C opsins, respectively (fig. 5). When Q122E was introduced to the RH2-C template, +16 nm of spectral shift was observed, explaining two-thirds of the spectral difference (fig. 6*C*). In contrast, there was no or only small additional spectral effects detected in other sites when mutations were introduced individually together with Q122E (fig. 6*C*) although we failed to reconstitute a measurable photopigment for L95I/Q122E.

At the site 123, two residues (V and I) are perfectly conserved in RH2-B and RH2-C opsins, respectively, as in the adjacent site 122 with a large spectral effect. When all but site 123 were replaced in the RH2-C template to the RH2-B types, the $\lambda_{max}$ matched well with that of RH2-B (supplementary fig. S5*A* and *B*, Supplementary Material online), confirming no effect of the site 123. Despite no spectral effect, the perfect conservation at the site 123 could be due to a hitchhiking effect by the close vicinity from the site 122. When other sites than the 123 and one additional sites (other than the site 122) were replaced in the RH2-C template to the RH2-B types, the $\lambda_{max}$ approached well to that of RH2-B (supplementary fig. 5*B*, Supplementary Material online), supporting individually small spectral effects of other sites than the site 122. In particular, no effect was detected for sites 205 and 270 (supplementary fig. 5*B*, Supplementary Material online).

To confirm whether the site 205 has no spectral effect, we replaced all but site 205 in the RH2-C template to the RH2-B types. The $\lambda_{max}$ matched with that of RH2-B (supplementary fig. 5*C*, Supplementary Material online), confirming that the site 205 has no effect. Using the RH2-C as the template,

when other sites than the 123 and 205 sites together with one additional site were replaced to the RH2-B types, the $\lambda_{max}$ differed slightly from that of RH2-B although we failed to evaluate the effect of site 96 (supplementary fig. 5*C*, Supplementary Material online). This shows individually small spectral effects of these additional sites including site 270 of which spectral effect was not detectable in supplementary figure 5*B*, Supplementary Material online.

These results suggest that the spectral difference between RH2-B and RH2-C opsins in genus *Oryzias* is maintained largely by the amino acid difference at site 122 and additionally by collective effects from amino acid differences at sites including 95, 96, 209, 213, and 270 through natural selection against gene conversion.

## Discussion

In the present study, we examined the green-sensitive *RH2-A*, *RH2-B*, and *RH2-C* opsin genes for orthologous and paralogous divergence at nucleotide sequence and at absorption spectrum of encoding photopigments among medaka fish, genus *Oryzias*, which are broadly distributed in fresh and brackish waters of Asia. Among six species studied, representing all three species groups *latipes*, *celebensis*, and *javanicus*, absorption spectra of RH2-A photopigments were divergent ($\lambda_{max}$ at 447–469 nm). Spectral divergence among the *Oryzias* RH2-A is caused largely (−15 nm) by a single amino acid replacement (T94C) and by collection of individually small effects. The T94C occurred in the phylogenetic branch leading to the *latipes* species group. This replacement appears to be driven by positive natural selection. Absorption spectra of RH2-B and RH2-C were distinct between the two opsins and conservative among species ($\lambda_{max}$ at 516–519 and 486–493 nm, respectively) despite that tracts of gene conversion were found to have homogenized the two genes. We showed that the spectral differentiation was realized largely by a single E/Q amino acid difference at the site 122 and by the collective effect from other sites with individually small spectral effects which are considered to be maintained by natural selection against the homogenization effect of gene conversion.

The amino acid site 122 is located in the transmembrane region surrounding the retinal and directly interacts with $\beta$-ionone ring of the 11-*cis* retinal (Ahuja et al. 2009). Amino acid replacements at the site 122 are known to cause large spectral shifts to RH1 (rhodopsins; dim-light-sensitive visual opsins produced in rod photoreceptor cells in the retina), RH2, and SWS2 opsins of diverse vertebrates (Sakmar et al. 1989; Yokoyama et al. 1999; Takahashi and Ebrey 2003; Chinen et al. 2005a). Similarly, the amino acid site 94 is in the close vicinity of the Schiff base linkage of the 11-*cis* retinal to K294 and its counterion E113 (Palczewski 2000). The spectral shift by T94C is probably via a direct electrostatic effect on the retinal chromophore (Takahashi and Ebrey 2003). The amino acid replacements S94A and C94A are reported to cause −14- and −16-nm shift to the SWS2 opsins of newt and bluefin killifish, respectively (Takahashi and Ebrey 2003; Yokoyama et al. 2007). However, when the S94A is introduced into the goldfish SWS2 opsin, it only causes −3-nm shift (Chinen et al. 2005b), suggesting that the spectral effect at the site 94 depends largely on the background amino acid sequence.

Whereas spectral effects of amino acid replacements at the sites 94 and 122 were relatively clear, effects of remaining replacements were not in the three RH2 subtypes in this study. Collective effects from multiple amino acid changes are often not additive. Additivity, exemplified by the "five-sites" rule of the M/LWS opsins (Yokoyama et al. 2008), is rather exceptional. This makes prediction of $\lambda_{max}$ unreliable based on empirical association of reported amino acid compositions at particular amino acid sites and observed $\lambda_{max}$ values (Chinen et al. 2005a, 2005b; Matsumoto et al. 2014; Kawamura et al. 2016). Recently, prediction of $\lambda_{max}$ values was made based on the magnitude of selected angles in carbon bonds in the conformation of 11-*cis* retinal under various amino acid sequence environments with known $\lambda_{max}$, as measured within atomistic molecular simulations (Patel et al. 2018). Accuracy of the prediction can be improved as more and more examples of observed $\lambda_{max}$ values for amino acid sequences are accumulated. Our present data should be a valuable source for the improvement.

In zebrafish, expression of *RH2-1* and *RH2-2* opsin genes, of which $\lambda_{max}$ values are the shortest and the second shortest among the four RH2 opsins, initiates earlier than the longer wave subtypes (Takechi and Kawamura 2005). Expression of zebrafish LWS opsin genes is similar, with the shorter wave-sensitive *LWS-2* expressed earlier than *LWS-1* (Takechi and Kawamura 2005). This chromatic organization of the larval zebrafish retina appears to fit well with the behavioral requirements for feeding on zooplankton in a shallow water column which shows enhanced contrast under the rich shorter wavelength of light in the natural environment (Novales Flamarique 2016; Zimmermann et al. 2018). Cichlids also express the different RH2 opsin genes depending on their growth stage and ambient light (Parry et al. 2005; Spady et al. 2006). The quantitative-PCR analysis for the adult retina showed that in *O. latipes*, the *RH2-A* and *RH2-B* were expressed at a higher level than *RH2-C* (Matsumoto et al. 2006). In comparison to zebrafish and cichlids, data for medaka are wanting on the spatiotemporal expression of these genes in the retina as well as difference of feeding ecology among species and among species groups at larval to adult stages. Our finding of the large variation of the shortest-wave-sensitive RH2-A among the RH2 subtypes should facilitate relevant studies at organismal and ecological levels.

$\lambda_{max}$ values of RH2-B and RH2-C opsins were found to be strictly conserved against homogenization effect by the gene conversion between their genes. The gene conversion and the

spectral conservation are also reported for primate LWS and MWS opsins (Balding et al. 1992; Hiwatashi et al. 2011). In primates, this spectral separation maintains the trichromatic color vision (Hiwatashi et al. 2011). However, it remains to be elucidated if the maintenance of spectral separation between the RH2-B and RH2-C opsins in medaka is for maintenance of color vision in which the two opsins are involved.

The effect of gene conversion on the divergence between duplicated genes has been well studied. A theoretical model demonstrates that the process consists of three phases I–III. Phase I is the time during which divergence reaches its equilibrium value. In phase II, divergence fluctuates around the equilibrium, and divergence increases again in phase III (Teshima and Innan 2004). The gene conversion was not observed between the *RH2-A* and the *RH2-B/C* genes. Gene duplication that derived the *RH2-A* gene and the ancestral *RH2-B/C* gene is ancient, predating speciation among Acanthopterygii (∼140 Ma) (Matsumoto et al. 2006; Betancur-R et al. 2017; Hughes et al. 2018). Thus, it is probable that the divergence between *RH2-A* and *RH2-B/C* has already been in the phase III.

Our analysis for the RH2 opsins of six medaka species (*O. latipes*, *O. luzonensis*, *O. celebensis*, *O. saracinorum*, *O. minutillus*, *and O. melastigma*) implied that all three subtype genes were retained by natural selection among the genus medaka and were functionally important. This is the first case that opsins among closely related congeneric species are reconstituted in vitro and compared for their absorption spectra. Medaka is an excellent model for examining the relationship between vision and photonic environments because of their diversity of photic environment and feasibility of laboratory studies. In future work, more detailed analyses of spatiotemporal gene expression in the retina are required for opsin genes of congeneric medaka species. Such studies would further clarify how fishes use multiple opsin genes formed by gene duplications and have adapted to their photic environments during evolution.

## Supplementary Material

Supplementary data are available at *Genome Biology and Evolution* online.

## Acknowledgments

We are grateful to NBRP Medaka for providing *Oryzias luzonensis*, *O. celebensis*, *O. sarasinorum*, *O. melastigma*, and *O. minutillus*. We thank Dr Deborah L. Stenkamp for proofreading and commenting on the article. Funding was provided by the Grants-in-Aid for Scientific Research (A) from the Japan Society for the Promotion of Science (JSPS) (15H02421 and 18H04005) to S.K. and the Grant-in-Aid for JSPS Fellows (06J11170) to Y.M.

## Author Contributions

S.K. designed research. Y.M. performed research and analyzed data. H.M. and S.O. contributed research materials. Y.M. and S.K. wrote the article.

## Literature Cited

Ahuja S, et al. 2009. Location of the retinal chromophore in the activated state of rhodopsin. J Biol Chem. 284(15):10190–10201.
Balding DJ, Nichols RA, Hunt DM. 1992. Detecting gene conversion: primate visual pigment genes. Proc Biol Sci. 249(1326):275–280.
Betancur-R R, et al. 2017. Phylogenetic classification of bony fishes. BMC Evol Biol. 17(1):162.
Carleton KL, et al. 2008. Visual sensitivities tuned by heterochronic shifts in opsin gene expression. BMC Biol. 6(1):22.
Chinen A, Hamaoka T, Yamada Y, Kawamura S. 2003. Gene duplication and spectral diversification of cone visual pigments of zebrafish. Genetics 163(2):663–675.
Chinen A, Matsumoto Y, Kawamura S. 2005a. Reconstitution of ancestral green visual pigments of zebrafish and molecular mechanism of their spectral differentiation. Mol Biol Evol. 22(4):1001–1010.
Chinen A, Matsumoto Y, Kawamura S. 2005b. Spectral differentiation of blue opsins between phylogenetically close but ecologically distant goldfish and zebrafish. J Biol Chem. 280(10):9460–9466.
Dayhoff MO, Schwartz RM, Orcutt BC. 1978. A model of evolutionary change in proteins. In: Dayhoff MO, editor. Atlas of protein sequence and structure. Silver Spring (MD): National Biomedical Research Foundation. p. 345–352.
Felsenstein J. 1985. Confidence limits on phylogenies – an approach using the bootstrap. Evolution 39(4):783–791.
Formacion MJ, Uwa H. 1985. Cytogenetic studies on the origin and species differentiation of the Philippine medaka, *Oryzias luzonensis*. J Fish Biol. 27(3):285–291.
Fuller RC, Carleton KL, Fadool JM, Spady TC, Travis J. 2004. Population variation in opsin expression in the bluefin killifish, *Lucania goodei*: a real-time PCR study. J Comp Physiol A. 190(2):147–154.
Hiwatashi T, et al. 2011. Gene conversion and purifying selection shape nucleotide variation in gibbon L/M opsin genes. BMC Evol Biol. 11(1):312.
Hughes LC, et al. 2018. Comprehensive phylogeny of ray-finned fishes (Actinopterygii) based on transcriptomic and genomic data. Proc Natl Acad Sci U S A. 115(24):6249–6254.
Iwamatsu T, Hamaguchi S, Naruse K, Takata K, Uwa H. 1993. Stocks of *Oryzias* species in Japan. Fish Biol J Medaka. 5:5–10.
Jones DT, Taylor WR, Thornton JM. 1992. The rapid generation of mutation data matrices from protein sequences. Comput Appl Biosci. 8(3):275–282.
Kasagi S, et al. 2015. Molecular and functional characterization of opsins in barfin flounder (*Verasper moseri*). Gene 556(2):182–191.
Kasahara M, et al. 2007. The medaka draft genome and insights into vertebrate genome evolution. Nature 447(7145):714–719.
Katsumura T, et al. 2009. Genetic differentiation among local populations of medaka fish (*Oryzias latipes*) evaluated through grid- and deme-based sampling. Gene 443(1–2):170–177.
Kawamura S, et al. 2016. Spectral sensitivity of guppy visual pigments reconstituted in vitro to resolve association of opsins with cone cell types. Vision Res. 127:67–73.
Kawamura S, Yokoyama S. 1998. Functional characterization of visual and nonvisual pigments of American chameleon (*Anolis carolinensis*). Vision Res. 38(1):37–44.
Kumar S, Stecher G, Li M, Knyaz C, Tamura K. 2018. MEGA X: molecular evolutionary genetics analysis across computing platforms. Mol Biol Evol. 35(6):1547–1549.

Mackin RD, et al. 2019. Endocrine regulation of multichromatic color vision. Proc Natl Acad Sci U S A. 116(34):16882–16891.
Matsumoto Y, et al. 2009. Medaka: a promising model animal for comparative population genomics. BMC Res Notes. 2(1):88.
Matsumoto Y, et al. 2014. Evolutionary renovation of L/M opsin polymorphism confers a fruit discrimination advantage to ateline New World monkeys. Mol Ecol. 23(7):1799–1812.
Matsumoto Y, Fukamachi S, Mitani H, Kawamura S. 2006. Functional characterization of visual opsin repertoire in Medaka (*Oryzias latipes*). Gene 371(2):268–278.
Matsuyama K. 1994. World Medaka aquarium in Nagoya Higashiyama Zoo. Fish Biol J Medaka. 6:57–60.
Musilova Z, et al. 2019. Vision using multiple distinct rod opsins in deep-sea fishes. Science 364(6440):588–592.
Nakamura Y, et al. 2013. Evolutionary changes of multiple visual pigment genes in the complete genome of Pacific bluefin tuna. Proc Natl Acad Sci U S A. 110(27):11061–11066.
Naruse K. 1996. Classification and phylogeny of fishes of the genus *Oryzias* and its relatives. Fish Biol J Medaka. 8:1–9.
Novales Flamarique I. 2016. Diminished foraging performance of a mutant zebrafish with reduced population of ultraviolet cones. Proc R Soc B. 283(1826):20160058.
Palczewski K. 2000. Crystal structure of rhodopsin: a G protein-coupled receptor. Science 289(5480):739–745.
Parenti LR. 2008. A phylogenetic analysis and taxonomic revision of ricefishes, *Oryzias* and relatives (Beloniformes, Adrianichthyidae). Zool J Linn Soc. 154(3):494–610.
Parenti LR, Soeroto B. 2004. *Adrianichthys roseni* and *Oryzias nebulosus*, two new ricefishes (Atherinomorpha: Beloniformes: Adrianichthyidae) from Lake Poso, Sulawesi, Indonesia. Ichthyol Res. 51(1):10–19.
Parry JW, et al. 2005. Mix and match color vision: tuning spectral sensitivity by differential opsin gene expression in Lake Malawi cichlids. Curr Biol. 15(19):1734–1739.
Patel JS, Brown CJ, Ytreberg FM, Stenkamp DL. 2018. Predicting peak spectral sensitivities of vertebrate cone visual pigments using atomistic molecular simulations. PLoS Comput Biol. 14(1):e1005974.
Rennison DJ, Owens GL, Taylor JS. 2012. Opsin gene duplication and divergence in ray-finned fish. Mol Phylogenet Evol. 62(3):986–1008.
Roberts TR. 1998. Systematic observations on tropical Asian medakas or ricefishes of the genus *Oryzias*, with descriptions of four new species. Ichthyol Res. 45(3):213–224.
Saitou N, Nei M. 1987. The neighbor-joining method: a new method for reconstructing phylogenetic trees. Mol Biol Evol. 4(4):406–425.
Sakmar TP, Franke RR, Khorana HG. 1989. Glutamic acid-113 serves as the retinylidene Schiff base counterion in bovine rhodopsin. Proc Natl Acad Sci U S A. 86(21):8309–8313.
Sawyer S. 1989. Statistical tests for detecting gene conversion. Mol Biol Evol. 6(5):526–538.
Setiamarga DH, et al. 2009. Divergence time of the two regional medaka populations in Japan as a new time scale for comparative genomics of vertebrates. Biol Lett. 5(6):812–816.
Spady TC, et al. 2006. Evolution of the cichlid visual palette through ontogenetic subfunctionalization of the opsin gene arrays. Mol Biol Evol. 23(8):1538–1547.
Takahashi Y, Ebrey TG. 2003. Molecular basis of spectral tuning in the newt short wavelength sensitive visual pigment. Biochemistry 42(20):6025–6034.
Takechi M, Kawamura S. 2005. Temporal and spatial changes in the expression pattern of multiple red and green subtype opsin genes during zebrafish development. J Exp Biol. 208(7):1337–1345.
Takehana Y, Nagai N, Matsuda M, Tsuchiya K, Sakaizumi M. 2003. Geographic variation and diversity of the cytochrome *b* gene in Japanese wild populations of medaka, Oryzias latipes. Zoolog Sci. 20(10):1279–1291.
Takehana Y, Naruse K, Sakaizumi M. 2005. Molecular phylogeny of the medaka fishes genus *Oryzias* (Beloniformes: Adrianichthyidae) based on nuclear and mitochondrial DNA sequences. Mol Phylogenet Evol. 36(2):417–428.
Tamura K, Nei M. 1993. Estimation of the number of nucleotide substitutions in the control region of mitochondrial DNA in humans and chimpanzees. Mol Biol Evol. 10(3):512–526.
Teshima KM, Innan H. 2004. The effect of gene conversion on the divergence between duplicated genes. Genetics 166(3):1553–1560.
Thompson JD, Higgins DG, Gibson TJ. 1994. CLUSTAL W: improving the sensitivity of progressive multiple sequence alignment through sequence weighting, position-specific gap penalties and weight matrix choice. Nucleic Acids Res. 22(22):4673–4680.
Watson CT, et al. 2011. Gene duplication and divergence of long wavelength-sensitive opsin genes in the guppy, *Poecilia reticulata*. J Mol Evol. 72(2):240–252.
Wittbrodt J, Shima A, Schartl M. 2002. Medaka–a model organism from the far East. Nat Rev Genet. 3(1):53–64.
Yang Z. 2007. PAML 4: phylogenetic analysis by maximum likelihood. Mol Biol Evol. 24(8):1586–1591.
Yang Z, Dos Reis M. 2011. Statistical properties of the branch-site test of positive selection. Mol Biol Evol. 28(3):1217–1228.
Yang Z, Kumar S, Nei M. 1995. A new method of inference of ancestral nucleotide and amino acid sequences. Genetics 141(4):1641–1650.
Yokoyama S. 2000. Molecular evolution of vertebrate visual pigments. Prog Retin Eye Res. 19(4):385–419.
Yokoyama S, Tada T. 2010. Evolutionary dynamics of rhodopsin type 2 opsins in vertebrates. Mol Biol Evol. 27(1):133–141.
Yokoyama S, Takenaka N, Blow N. 2007. A novel spectral tuning in the short wavelength-sensitive (SWS1 and SWS2) pigments of bluefin killifish (*Lucania goodei*). Gene 396(1):196–202.
Yokoyama S, Yang H, Starmer WT. 2008. Molecular basis of spectral tuning in the red- and green-sensitive (M/LWS) pigments in vertebrates. Genetics 179(4):2037–2043.
Yokoyama S, Zhang H, Radlwimmer FB, Blow NS. 1999. Adaptive evolution of color vision of the Comoran coelacanth (*Latimeria chalumnae*). Proc Natl Acad Sci U S A. 96(11):6279–6284.
Zimmermann MJY, et al. 2018. Zebrafish differentially process color across visual space to match natural scenes. Curr Biol. 28(13):2018–2032.

**Associate editor:** Yoko Satta